Available online at www.sciencedirect.com
SCIENCE DIRECT®
Planetary and Space Science 51 (2003) 953–961
Planetary and Space Science
www.elsevier.com/locate/pss

Water ice on outer solar system surfaces: Basic properties and radiation effects

Raúl A. Baragiola*

Laboratory for Atomic and Surface Physics, Engineering Physics, University of Virginia, 116 Engineers Way, Charlottesville, VA 22904-4238, USA

Received 17 December 2002; received in revised form 5 May 2003; accepted 12 May 2003

Abstract

This paper reviews the properties of vapor-deposited water ice in connection with icy surfaces in the outer solar system. The emphasis is on knowledge gained during the last decade, and on the properties of the amorphous phase, especially those affected by the presence of microporosity. The paper discusses the role played by the properties of different phases of ice and the effect of irradiation on the icy surfaces of satellites in the outer solar system: sputtering, phase transformation, the production and trapping of molecular radiation products, and stress induced cracking. The understanding of how growth and irradiation processes affect the optical properties of ice will lead to extract better information from optical remote sensing than is possible today. It is argued that cracks in ice induced by stresses are the main reason causing low-temperature ices to be strongly scattering.

Keywords: Absorption; Cracking; Europa; Irradiation; Radiolysis

1. Introduction

This paper is focused on describing results from the past decade on the properties of vapor-deposited water ice and astronomical implications, with emphasis on the microporous amorphous phase (amorphous solid water or ASW), which is believed to be the most abundant form of water in the universe. In the solar system, vapor-deposited water ice, in the amorphous or cubic phases, is the principal constituent of the surface of many satellites and rings (Schmitt et al., 1998a). Water coexists with other condensed gases, and mixed with mineral grains. Most of our knowledge about these icy surfaces comes from studies of the reflected solar light. The sampled depth (optical skin) in optical reflectance varies with wavelength. In the infrared, this depth is of the order of microns or less, while in the near ultraviolet to near infrared range, it can be centimeters or more (limited by a combination of scattering and absorption by non-ice material, e.g., minerals). The optical skin is subject to bombardment by energetic particles and Lyman-α radiation from the Sun, planetary magnetospheric ions, cosmic rays, and meteorites (Johnson, 1998). These energetic impacts induce many effects on the ice surface, like chemical reactions, electrostatic charging, lattice damage, desorption, and evaporation, some of which alter the appearance of the surface.

Within the spatial resolution of the optical observations, surface ices are likely very inhomogeneous. The ejection of molecules from thermal sublimation, sputtering, and micrometeorite impact mostly redistributes ice on the surface in the presence of sufficient gravity. The fraction of gravitationally bound ejecta will be large on a massive object like Ganymede and negligible on an icy ring particle. All these processes contribute to the formation of a yet unknown icy microstructure which should differ from the regolith of rocky airless bodies due to the higher propensity for molecular motion afforded by the lower cohesive forces of water.

A crucial characteristic of vapor-deposited amorphous water ice is its microporosity, which affects most other properties. Since pore dimensions are smaller than optical wavelengths (down to ~ 2 nm) microporosity does not contribute appreciably to optical scattering. It may, however, be assessed by careful measurements of infrared reflectance spectra (see below). Microporosity produces large effective surface areas for gas absorption that can reach several hundred m^2/g for ice grown at very low temperatures (< 100 K).

* Tel.: +1-804-922-2907; fax: +1-804-924-1353.
E-mail address: raul@virginia.edu (R.A. Baragiola).

0032-0633/$ - see front matter © 2003 Elsevier Ltd. All rights reserved.
doi:10.1016/j.pss.2003.05.007

Thus, a fresh ASW surface acts like a high-capacity vacuum pump. This pumping ability and long exposure times mean that icy surfaces in the outer solar system may be saturated with atmospheric gases. In laboratory studies, it means that contamination will be present to an extent that depends on experimental conditions. Far from saturation adsorption on the surface area of the pores, the degree of ice contamination is proportional to Pt/d, the surface exposure to gas, Pt, divided by the thickness d of the ice, where P is the pressure and t the exposure time. Particularly susceptible to contamination are experiments on ultrathin films (like those used in transmission electron microscopy) or long measurement times (like X-ray or neutron diffraction studies). Unfortunately, in the vast majority of the published laboratory reports there is no mention of chemical analysis or of the composition of background gases. Since contamination can affect properties of the amorphous deposits, it is sensible to speculate that varied vacuum conditions are a reason for the common large discrepancies in laboratory results found in the literature.

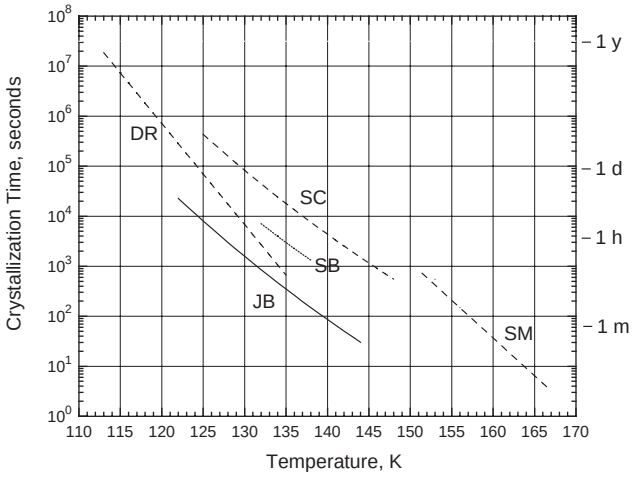

Fig. 1. Compendium of experimental data for crystallization times of vacuum-deposited amorphous ice; lines indicate fits to the data. Dashed line, start of the transformation: JB, Jenniskens and Blake (1996), Dotted line, 63% crystallized: SB, Sack and Baragiola (1993). End of transformation curves are shown as dashed lines: DR, Dowell and Rinfret (1960); SC, Schmitt et al. (1989); SM, Smith et al. (1996).

2. Phases of water ice at low pressures

Temperature is the main factor determining the crystallographic phase of ice grown from the gas phase at low pressures. The hexagonal phase (Ih) common on Earth is formed by condensation onto a substrate cooled to temperatures above $\sim$ 190 K. Condensation below 190 K but above $\sim$ 135 K, leads to cubic crystalline ice (Ic), which transforms into Ih if warmed above 160–200 K. Deposits formed on substrates colder than $\sim$ 130 K are amorphous, i.e., lacking long-range crystalline order while keeping local tetrahedral ordering (Sceats and Rice, 1982). The amorphous phase is metastable and converts to Ic at a rate that depends on temperature (Fig. 1). Both crystallization and the Ic→Ih transitions are thermally irreversible. This means that, in the absence of irradiation-induced phase transformations (see below), the phase of the surface ice on a given object will depend on its thermal history.

There are two clearly distinctive types of ASW grown from the vapor phase. The usual form has an intrinsic (local) density $\rho = 0.94$ g/cm^3. A high-density form ($\rho = 1.1$ g/cm^3 locally), grows at 10 K or below and transforms into the low-density ASW at $\sim$ 114 K (Handa et al., 1986; Jenniskens et al., 1995; Jenniskens and Blake, 1994, 1996). It is likely that a continuum of polymorphs form, as shown by infrared absorption spectra (Schriver-Mazzuoli et al., 2000).

The early studies of X-ray diffraction by Rice and co-workers, reviewed by Sceats and Rice (1982) produced the surprising finding that low condensation rates (less than a few monolayers/sec) produce ASW at < 110 K, and that high condensation rates produce Ic. This is unrelated to the release of heat of condensation, which is negligible at the condensation rates used in high-vacuum experiments (at one monolayer/sec the heat input is only 8.4×10^{-5} W/cm^2). The often quoted recipe of Olander and Rice (1972) to prepare fully amorphous ice is either to grow it below 55 K or to limit the growth rate to < 100 μm/h. This contrasts with expectations based on studies where amorphous solids are formed when the deposition is so fast that diffusion is unable to arrange the molecules in the more stable crystalline structure. Possibly low condensation rates allowed enough contaminants from the background gas to co-deposit on the film, distorting the lattice. Many later studies disagree with the prescription of Olander and Rice. For instance, Hagen et al. (1981) used infrared spectroscopy to infer that ice is more disordered at high deposition rates. Using more direct X-ray diffraction methods, Hallbrucker et al. (1989) grew $> 98\%$ amorphous films at 77 K at a rate two orders of magnitude faster than the Olander and Rice limit. The highest reported temperature at which amorphous growth (determined from the shape of the O–H infrared band) occurs is 145 K (Mitlin and Leung, 2002) with a growth rate of 1.5 μm/h.

Deposits of amorphous ice contain embedded crystalline grains in amounts that depend on temperature (Sack and Baragiola, 1993), and the smoothness of the substrate (Trakhtenberg et al., 1997). Unexpectedly, Moore et al. (1994) found that crystalline ice formed on small silicate grains below 20 K. A possible reason is localized heating due to the inability of the grains to dissipate the condensation energy.

Different types of amorphous ice can be produced by other methods. Rapid cooling of liquid water produces an amorphous phase called hyper-quenched glassy water (HGW) (Johari et al., 1987). This type of ice may be found on icy satellites when water liquefied in a meteorite impact solidifies rapidly. High pressures can amorphize Ih into the

high-density amorphous phase (HDA), with $\rho = 1.31$ g/cm^3 (Mishima et al., 1984). When the pressure is released, HDA transforms into the low-density amorphous phase (LDA), with $\rho = 1.17$ g/cm^3, through a continuum of amorphous structures (Tulk et al., 2002). A direct comparison has not been made between this phase and the high-density phase that forms by vapor deposition below 20 K, mentioned above. HDA and LDA may also form in high-pressure events induced by meteorite impacts, at sufficient distance from the impact crater such that heating does not induce crystallization.

2.1. Crystallization

Much confusion exists in the literature about the temperature for phase transformations in ASW. These transformations do not occur at a particular temperature, but continuously over a temperature range. In an experiment where ice is warmed up from a low temperature, crystallization will start at a lower temperature the lower the heating rate. In typical laboratory time scales, ASW crystallizes to Ic above 125 K. The total crystallization time, the sum of the nucleation time and the transformation time, has been measured with a variety of techniques. As shown in the composite plot (Fig. 1), most of the experiments agree over the wide range from start to finish of crystallization, from which one can derive an activation energy of ~ 0.4 eV. Some spread is expected from different ways of preparing the ASW films that result in different contents of micropores and crystalline grains (Sack and Baragiola, 1993; Dohnálek et al., 2000) and from the sensitivity of the different techniques to identify the start and finish of crystallization.

Several reports indicate that ASW does not crystallize completely in the range 130–150 K (Dowell and Rinfret, 1960; Hagen et al., 1983; Hallbrucker et al., 1989; Hessinger et al., 1996). Jenniskens and Blake (1994) and Jenniskens et al. (1997) found that in very thin films, ASW exists inside Ic at temperatures higher than those quoted for crystallization. These results differ from those using different techniques. Kohl et al. (2000), using X-ray diffraction, found that HGW annealed to 183 K contains at most 20% amorphous component, quite lower than that reported by Jenniskens et al. On the other hand, sublimation rates fall to the values of crystalline ice at ~ 140 K (Sack and Baragiola, 1993; La Spisa et al., 2001) suggesting that only a negligible contribution of ASW can remain since sublimation from ASW is about two orders of magnitude larger than for Ic.

3. Optical absorption spectra

There are several reviews of infrared spectra of water ice (Sceats and Rice, 1982; Hudgins et al., 1993; Devlin, 1990); see also later work by Wojcik et al. (1993), Langel et al. (1994), Moore and Hudson (1992, 1993), Smith et al. (1994) and Moore et al. (2001). Fig. 2 depicts optical constant of ASW and Ic at different temperatures. The spectra consist of intense bands with absorbance that peaks approximately at 3.1 μm (O–H stretch), 6.1 μm (bending), 12 μm (libration), the lattice modes above 20 μm (peaking at 46 μm), and a combination band at 4.6 μm. Not shown are the weak overtones at 2, 1.5, and 1.0 μm, which are useful for determining optical skin depths in remote sensing of icy satellites.

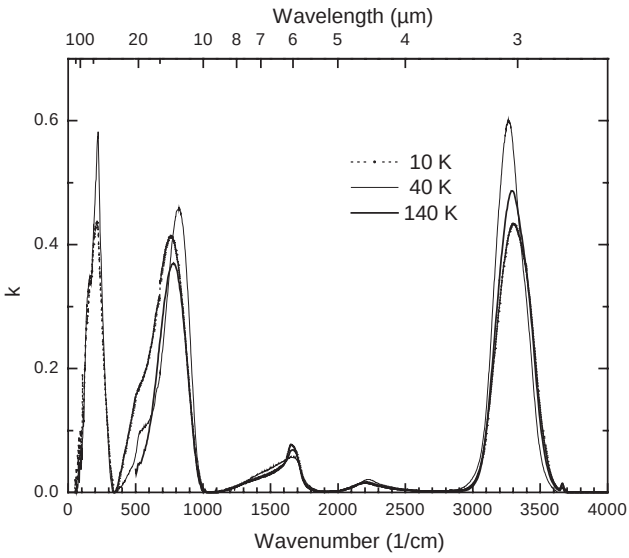

Fig. 2. Imaginary part of the index of refraction k of amorphous ice deposited at 10 K, and after annealing to 40 and 140 K (Hudgins et al., 1993).

The infrared absorption band most used in astronomical observations is the vibration of the O–H stretch. It has diagnostic value since it is prominently wider in ASW than in Ic but unfortunately this band is saturated in many icy bodies. The types of disorder that contribute to the bandwidth in ASW are the proton disorder (also present in Ic), the disorder in the oxygen positions, and the micropores. The latter contribution, not considered in the early spectral analysis (Sceats and Rice, 1982), is deduced from the narrowing of the bands when ice is annealed (compacted) without crystallization (see below). The variation of the absorption band shape and position with temperature is useful to diagnose astronomical ices (Hagen et al., 1983; Léger et al., 1983; Schmitt et al., 1998b; Grundy et al., 1999). Also diagnostic are the very distinct variations with temperature (Fig. 2) and phase (Bertie et al., 1969; Hudgins et al., 1993) in the mid- and far-IR and the sharp absorption at 2.71 μm due to the O–H vibrational stretch in dangling bonds (Rowland et al., 1991), which shifts in frequency when gas is adsorbed, and becomes weaker during annealing.

4. Microporosity of ASW

Based on cluster calculations, Buch (1992) proposed that the reason ASW is microporous is that incoming molecules

attach preferentially to dangling bonds sticking out of the surface and thus stick out even more, forming increasingly longer surface protrusions. Already simpler "hit and stick" models, with crude or simplified intermolecular potentials give an open structure, with porosity increasing with the angle of incidence of the incoming water flux (Essmann and Geiger, 1995; Zhdanov and Norton, 2000; Kimmel et al., 2001). The fact that limited microporosity results during growth even at relatively high temperatures close to the crystallization transition suggests that diffusion during deposition is negligible.

Experimentally, the porosity of ASW may be derived directly from measurements of the density of the films or of the index of refraction, related to porosity by the Lorentz–Lorenz relation. Westley et al. (1998) have reviewed recently measurements of the density and porosity of ASW. The intrinsic density (local, not including micropores) $\rho \sim 0.94$ g/cm^3 is derived from the O–O distance measured with X-ray diffraction (Sceats and Rice, 1982).

Optical measurements yield a lower bulk density, which includes pore space. Densities can be as low as ~ 0.6 g/cm^3 at 20 K, when the films are grown with omni directional water flux from a relatively high ambient water pressure. Westley et al. (1998) proposed that the wide range of reported densities is due to the change of porosity with angle of incidence of the incident water flux with respect to the substrate, which is different in different experiments. The idea was recently confirmed in density measurements in our laboratory (Sekar and Baragiola, to be published), and is consistent with the finding by Stevenson et al. (1999) of a dependence of gas absorption capacity (indicative of the open porosity) on deposition angle.

5. Gas absorption and retention

Studies of gas absorption give information useful to model astronomical processes and help characterize the pores connected to the outside of the ice, but not the enclosed pores (which cannot trap gas, except for radiation products). If multilayers are not formed, measurements of the amount of gas absorbed can be used to obtain the total absorption area of the solid. For microporous solids, the total area is essentially the internal surface area unless the measurements use very thin and rough films. Absorption areas can be hundreds of m^2/g, and decrease with growth and annealing temperatures. Thermal desorption studies show a similar behavior for gas co-deposited with water or dosed on the ASW. Desorption occurs in distinct peaks as a function of temperature, many of which appear related to phase transformations. Classical absorption isotherm studies give information on pore size. Mayer and Pletzer (1986) inferred that a small fraction of pores are wider than 2 nm while Schmitt et al. (1987), comparing N_2 and Ar absorption in ASW, concluded that most pores are only a few molecular diameters wide.

Extensive investigations of gas absorption in ASW have been done by Bar-Nun and colleagues (Bar-Nun and Owen, 1998), to understand the trapping and release of gases in comets. The work established several distinct temperature regions for gas release, beyond the peaks occurring at crystallization and at the Ic→Ih transition, and that the temperatures at which gas release peaks depend on heating rate. The effective surface area for gas absorption increases with the angle of incidence of water during condensation (Stevenson et al., 1999), consistent with the increased porosity predicted by Westley et al. (1998).

With increasing growth temperature, the gas absorption ability or open porosity of ASW decreases strongly (Brown et al., 1996; Stevenson et al., 1999; Vichnevetski et al., 2000; Horimoto et al., 2002). In particular, Rowland et al. (1991) found that dangling bonds already diminish upon warming to 60 K while Stevenson et al. (1999) could not detect absorption due to open micropores in ice grown at above 90 K. This indicates that micropores that remain in the ice above 60 K are closed to gas access through the surface. There is clearly the need to identify the fraction of pores that remain in the ice (which affect mechanical properties), without connection to the outside.

Warming ice at a temperature higher than the deposition temperature, but below the onset for crystallization, produces irreversible exothermic changes (annealing). These are not well understood, particularly below 115 K, where diffusion is insignificant (Fisher and Devlin, 1995). Annealing causes changes in X-ray diffraction (Hallbrucker et al., 1989) and irreversible narrowing and shifts of the O–H infrared band (e.g., Hagen et al., 1981; Drobyshev and Garipoglyi, 1996; Givan et al., 1997; Jenniskens et al., 1997; Schmitt et al., 1998b; Schriver-Mazzuoli et al., 2000). Eldrup et al. (1985) used positron annihilation techniques to establish that ~ 1.7 nm cavities in ASW disappear or coalesce at 100 K, but that some persist even after warming past crystallization. Annealing makes ASW more compact by closing pores thereby decreasing the gas absorption ability and other properties (Johari et al., 1991; Tsekouras et al., 1998; Giering and Haarer, 1996). Bar-Nun et al. (Bar-Nun and Owen, 1998) found that the surface area for absorption decreased by $\sim 90\%$ when the ASW film was heated from 10–20 K to 122 K. Schmitt et al. (1987) found a similar decrease of gas trapping ability and a slow decrease in the absorption area time for a film grown at 77 K and kept at that temperature. Horimoto et al. (2002) combined methane absorption and infrared spectroscopy and concluded that cavities larger than micropores are responsible for gas absorption and that they collapse upon annealing to 60 K, whereas micropores are not affected until 80 K and disappear only at 120 K.

The effect of porosity on the mechanical properties of ice is evident in measurements of internal friction of ASW films. The decrease in internal friction between 20 and 84 K (Hessinger and Pohl, 1996) has been linked to a reduction of porosity and mostly to a reduction of local atomic disorder.

This annealing had a logarithmic dependence on time; it was not complete even after a 12 h at 126.6 K while maintaining a shear module half the bulk value for compact ice (White et al., 1998).

A common view is emerging from the literature. It appears that ice grown or annealed near crystallization temperatures still contain a porosity of 0.05–0.1 (void fraction), while the internal area for gas absorption is lower by more than an order of magnitude compared with ice that has not been heated above 60–80 K. The residual porosity remaining after warming the ice, not accompanied by a large absorption area, mean that annealing has the effect of disconnecting the pores from the surface so they become inaccessible to molecules from the outside. The implication of these results for the icy satellites is not yet clear, and must await measurements where gas is deposited together with water, to simulate the synergy of sublimation and sputtering with gas absorption from an atmosphere.

6. Optical reflectance

Optical reflectance is still the source of most of what we know about extraterrestrial icy objects (see, e.g., reviews by Hapke, 1983, and by Verbiscer and Helfenstein, 1998). Defect free, pure ice is transparent and reflects very little light. Laboratory prepared thin ASW or crystalline ice films scatter very little light (Westley et al., 1998) since micropores and grain boundaries are much smaller than the wavelength of light. Cracks, wide boundaries between particles, and surface topography on a scale comparable or larger than the wavelength of light can strongly affect optical reflectance. There are conflicting reports on the question of the scale of roughness of laboratory-grown surfaces. Very little is known about the development of topography during growth. Laufer et al. (1987) found needle structures on pure and gas-filled amorphous films condensed below 100 K, which persisted upon warming until the film disappeared at 180 K. Mayer and Pletzer (1986) found similar structures when using a gas doser in conditions allowing clustering of water molecules. Atteberry (1999) observed ice needles on the surface of vapor-deposited ice, but determined that they result from peculiar growth conditions that allowed deposition of ice pre-condensed on the gas doser.

Thin ASW films become white (frost-like) when heated over the crystallization temperature (Westley et al., 1998). All films grown on an optically flat gold surface are nearly invisible as long as the thickness is not so large as to cause cracking. The transition from transparent to frosty during growth at low temperatures has been seen in several studies (Wood and Roux, 1982; Schmitt et al., 1987; Bahr, 2000; Bahr and Baragiola, to be published). The critical thickness for cracking increases with growth temperature (Bahr, 2000) and with angle of incidence of the water molecules (Pugh, 2002). A transparent film may also crack during heating, due to thermal stresses and density variations during phase transformations (Westley et al., 1998). Cracking is also likely the cause of the abrupt increase in the optical reflectance seen by Drobyshev et al. (1993) and Drobyshev (1996) and in gas desorption (Smith et al., 1996).

Brown et al. (1978) and Strazzulla et al. (1988) observed that amorphous ice films brighten under ion irradiation. It has been speculated that this is due to scattering from defects induced by radiolysis. Since such small defects are unlikely to cause much scattering of optical light, this author feels that a more likely explanation is that defects produced by irradiation generate stresses that can trigger cracking of an already pre-stressed deposit. Films that have already cracked because they were grown below 60 K to a thickness larger than several microns become *less* reflecting under ion irradiation (Sack et al., 1991), as the molecular motions induced by the energetic ions partially fill in the cracks.

7. Thermal properties

Two unusual thermal properties of ASW are its low sublimation energy and low thermal conductivity. Both influence the stability and transport of ice in space. ASW found in astronomical bodies is not pristine. On the relatively warm icy Jovian satellites it is purified by fractionation due to sublimation: water desorbs from dirty (dark and therefore warm) regions and condenses on bright, cold regions. This distillation competes with compound formation due to ion implantation and mixing with debris from micrometeorite impact on mineral surfaces.

Kouchi (1987) discovered that the sublimation rate of ASW is much larger (up to two orders of magnitude) than for cubic ice, and that it depends on growth conditions. In his experiments the temperature of the ice was ramped linearly with time at 1 K/min while recording the flux of desorbed water with a mass spectrometer, a technique called temperature-programmed desorption (TPD). The sublimation rate shows a “bump” at temperatures about 135 K and decreases at higher temperatures to the rate appropriate to crystalline ice. This is shown in Fig. 3, obtained by Bahr and the author in measurements described in Bahr et al. (2001). The absolute isothermal sublimation rates measured by Sack and Baragiola (1993) showed a roughly exponential decrease of sublimation with time. They explained that the bump in TPD signals crystallization, and that it should occur at lower temperature when the heating rate is low. The implication of a higher sublimation rate for ASW than for cubic ice is that sublimation depends on the amorphous content of ice deposits (Sack and Baragiola, 1993). This means that the evolution of water from comets will be different on the first passage of the comet around the Sun than on subsequent orbits, since heating by the Sun induces crystallization in addition to sublimation.

The thermal conductivity of ice is needed to model the thermal inertia of icy surfaces. At low temperatures, the thermal conductivity is much smaller for amorphous than for

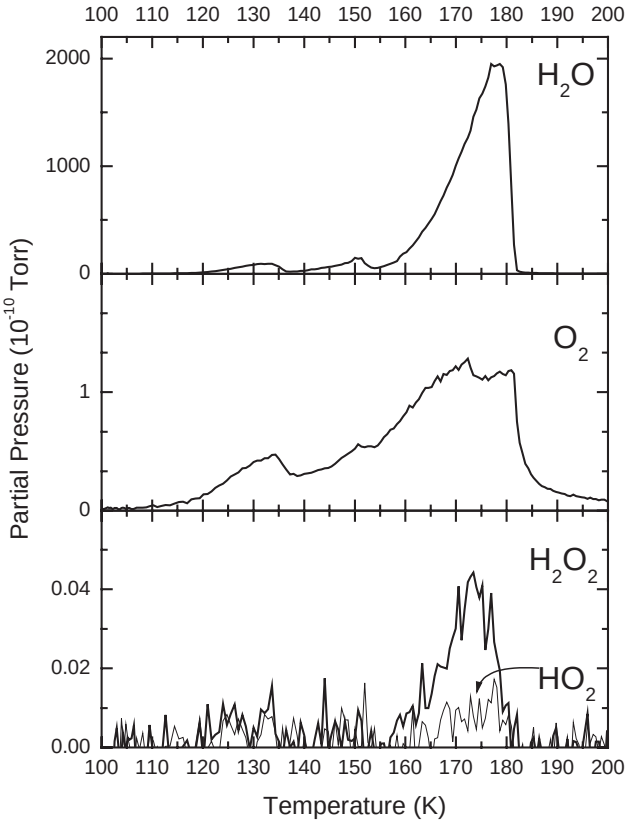

Fig. 3. Thermal desorption spectrum of a $\sim$ 7 μm ice film radiolyzed at 100 K with 1.5×10^{17} 200 keV protons/cm^2. The top graph, showing water desorption, is very similar to that of unirradiated ice, except for the small peak at $\sim$ 130 K correlated with oxygen emission. Note the bump at $\sim$ 150 K due to crystallization. Heating rate is $\sim$ 1.5 K/min. The fast drop near 180 K is due to the removal of the film. The two lower graphs for molecular species are obtained only after irradiation. The partial pressures are not corrected for the dependence of pumping speed and detection efficiency for different species.

crystalline solids and even lower if the solid is porous, due to increased phonon scattering. Kouchi et al. (1992) used an indirect electron beam technique to obtain an extremely low conductivity of ASW in a narrow temperature range (125–135 K), four or five orders of magnitude smaller than values for non-porous amorphous ice (Andersson and Suga, 1994). Baragiola (2003) has pointed out to errors in the thermal analysis of the experiment and to potential spurious effects of the high-energy electrons used. There is clearly a need for new measurements of thermal conductivity of ASW as a function of porosity.

8. Radiation-induced alterations

Irradiation of ice by energetic particles and photons is common in airless astronomical bodies. It produces radiation damage, chemical changes, the emission of atomic and molecular particles (desorption or sputtering), and the emission of electrons and luminescence photons. In addition to the observation of ejection of different particles and light, one can study chemical changes from measurements of infrared spectra, luminescence techniques and electron spectroscopy.

8.1. Radiolysis

Johnson and Quickenden (1997) have reviewed photolysis and radiolysis of ice. The primary molecular dissociation in water is OH + H. Plonka et al. (2000) have shown that OH radicals can be stored in ice up to temperatures of $\sim$ 130 K in crystalline ice and $\sim$ 100 K in hyperquenched glassy water (HGW). H atoms diffuse and recombine either with OH forming H_2O or with another H forming H_2, which can then escape from the solid. With increasing irradiation fluence, the concentration of OH radicals increases to a limit imposed by recombination with H and by reactions with other OH that yield H_2O_2. Fast ions produce a dense track of excitations in the solid; within this track the density of OH is high enough that hydrogen peroxide can be formed by a single ion.

Remote observation of long-lived radicals and stable molecular products of radiation can be studied in ice by infrared spectroscopy and comparison with laboratory studies (Gerakines et al., 1996). Moore and Hudson (2000) observed H_2O_2 formation in ice by 800 keV protons at 16 K, but not at 80 K. In contrast, Gomis et al. (to be published) detected H_2O_2 at 16 K but also at 77 K, this time using similar experiments using 30 keV protons. The discrepancy, which may be related to different excitation densities at the two energies, needs to be resolved to assess if this process can explain the observation of hydrogen peroxide at Europa (Carlson et al., 1999). Alternative ways of producing H_2O_2 on Europa are surface reactions with atmospheric atomic O, and ion irradiation of ice containing O_2. Mass spectrometry of gases released when heating radiolyzed ice also reveals the presence of O_2, H_2O_2, and HO_2 radiation products (Bahr et al., 2001), as shown in Fig. 3.

Solid molecular oxygen was detected on Ganymede from absorption bands in the visible (Spencer et al., 1995). This raised the question of how this solid O_2 can exist at the reported high surface temperatures if the vapor pressure would exceed the atmospheric pressure by many orders of magnitude. Johnson and Jesser (1997) have proposed that O_2 is formed inside the ice by radiolysis, and trapped in bubbles or inclusions. Our experiments confirmed that O_2 could be formed inside the ice by irradiation but not in sufficient quantities to explain the astronomical observations. In addition, O_2 cannot be trapped permanently but diffuses out of the ice at Ganymede's reported temperatures (Vidal et al., 1997). Transient trapping of oxygen in ice can be made by co-depositing O_2 and water in a film. When warmed above 70 K, the absorption bands become those of liquid oxygen, and different from those observed on Ganymede (Baragiola and Bahr, 1998). The explanation we suggested

is that oxygen can condense in very cold regions that exist on Ganymede, made of segregated, bright ice patches, undetectable by the Galileo infrared radiometer (Baragiola et al., 1999).

8.2. Phase transitions induced by irradiation

Crystalline ice can be amorphized by irradiation at temperatures below 70 K with high-energy electrons (Dubochet and Lepault, 1984), ions (Baratta et al., 1991; Moore and Hudson, 1992; Hudson and Moore, 1992, 1995), or 110–400 nm UV light (Kouchi and Kuroda, 1990; Leto and Baratta, 2003). Recrystallization upon heating leads to the original crystalline phase that was amorphized by the radiation, suggesting either a memory effect (Dubochet and Lepault, 1984) or growth from crystallites remaining from an incomplete amorphization (Mishima et al., 1984; Handa et al., 1986). Studies of amorphization by energetic ions have been based on changes in infrared absorption. Hudson and Moore (1992) observed an oscillation between crystalline and amorphous phases vs. irradiation fluence. Changes in the partial pressure of H_2 in the vacuum chamber, that accompanied these phase oscillations, could not be observed in other laboratories (Baratta et al., 1994; Leto et al., 1996; Baragiola et al., 2003). Another notable discrepancy is the incompatible results of amorphization by UV light by Kouchi and Kuroda (1990) and Leto and Baratta (2003).

In addition to amorphization of Ic at low temperatures, crystallization of ASW above 110 K can be induced by high-energy ions (Brown et al., 1978) or electrons (Heide, 1984).

9. Sputtering

Irradiation can produce the ejection of molecules that leads to the erosion of the surface either directly or through secondary electrons generated in ionizing collisions. In this paper sputtering is used as a synonym for impact desorption. Sputtering may lead to mass loss if the ejected atoms and molecules can escape the gravitational pull of the body, or it can lead to the redistribution of molecules on the surface. The ejected species form a transient water atmosphere that also interacts with the incoming radiation. For instance, the surfaces of the icy Jovian satellites are bombarded by magnetospheric ions with energies from eVs to MeVs, peaking at $\sim$ 100 keV (Johnson et al., 1998). Water molecules, H_2 and O_2 are ejected from the surface; in addition, neutral and charged H_2, O_2, H, O, O_3, H_2O_2, and HO_2 can be formed by interactions of the incoming radiation with the water atmosphere and subsequent chemical reactions. While relatively fast H_2 will predominantly escape gravity, water and oxygen molecules will mostly precipitate back onto the surface. Oxygen molecules that return to the surface may be trapped in the pores of the ice, or be scattered back to the atmosphere, resulting in a tenuous oxygen atmosphere around icy satellites. Trapping of O_2 depends strongly on ice porosity and temperature, which can go from a few Kelvin in permanently shielded regions to 160 K on the sub-solar regions of Callisto. Insufficient laboratory data exists currently to model the generation of water and oxygen atmospheres beyond order of magnitude estimates (Shi et al., 1995).

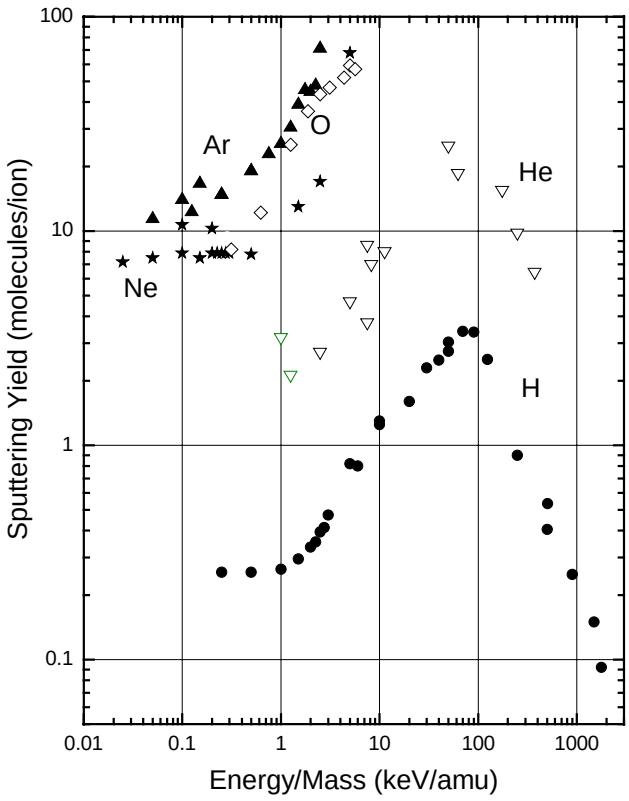

Fig. 4. Compilation of sputtering yields of ice vs. energy/amu of singly charged ions at normal incidence (Baragiola et al., 2003).

Sputtering is characterized by the sputtering yield, Y, the number of molecules or atoms ejected per incident projectile. There are two types of sputtering, depending on how energy is transferred from the projectile to the solid. Knock-on sputtering (Baragiola et al., 2003), due to the momentum transfer in close collisions, is not well understood for molecular insulators like water ice. It dominates sputtering of ice at low ion energies as evidenced in the "plateau" in the energy dependence of Y (Bar-Nun et al., 1985a; Shi et al., 1995; Baragiola et al., 2002, 2003) (Fig. 4). In electronic sputtering, the projectile transfers energy to the electronic system that leads to the formation of repulsive configurations in the solid. Brown et al. (1978) were the first to find the high electronic sputtering yields for water ice and show the astronomical implications.

The topic of sputtering of water ice was recently reviewed by Baragiola et al. (2003). Some features that are important to planetary science are summarized here. Sputtering yields are insensitive to ice growth conditions that lead to ASW or cubic ice (Bar-Nun et al., 1985b; Westley et al., 1995a). The

main species ejected are intact water molecules, with near thermal energies. The total sputtering yield stays essentially constant below 60–100 K and increases rapidly at higher temperatures. In the solar system, this temperature dependence is only important around Jupiter. In contrast, there is a strong temperature dependence of the partial sputtering yield of oxygen and hydrogen molecules, down to 10 K. These molecular species are also emitted during irradiation with 10.2 eV photons (Westley et al., 1995b) and low-energy electrons (Sieger et al., 1998; Wagner et al., 2002).

The ion-induced sputtering yield is proportional to the square of the electronic energy deposition near the surface, indicating that multiple collisions are important. In contrast, sputtering by 100–200 keV electrons in an electron microscope produces much lower sputtering yields that depend linearly on electronic energy deposition (Heide and Zeitler, 1985; Heide, 1982, 1984). Sputtering by single events occurs with incident Lyman-α photons (Westley et al., 1995a) and low-energy electrons (Kimmel et al., 1994; Rowntree et al., 1991).

10. Conclusions

Much progress has been done in the past decade in the understanding of the growth and properties of vapor-deposited water ice, for application to icy objects of the solar system. This paper has pointed out areas in which there exists the need for more laboratory data to model astronomical processes and explain astronomical observations. Among these areas are properties of ice in equilibrium with radiation and an atmosphere, and the creation of sufficient data and theoretical models that allow extrapolating from the laboratory to the astrophysical time scales. Different evidence on compaction of ice at temperatures where diffusion is negligible, points to the question of a possible weak time dependence that has not yet been detected in the laboratory but which may have astronomical implications.

Acknowledgements

We acknowledge financial support from the NASA's Planetary Geology and Geophysics Program, and the NSF Astronomy Division.

References

Andersson, O., Suga, H., 1994. Solid State Commun. 91, 985–988.
Atteberry, C., 1999. MS. Thesis, University of Virginia.
Bahr, D.A., 2000. Ph.D. Thesis, University of Virginia.
Bahr, D.A., Fama, M.A., Vidal, R.A., Baragiola, R.A., 2001. J. Geophys. Res. E 106, 33,285–33,290.
Baragiola, R.A., 2003. In: Devlin, J.P., Buch, B. (Eds.), Water in Confining Geometries. Elsevier, Amsterdam, in press.
Baragiola, R.A., Bahr, D.A., 1998. J. Geophys. Res. 103, 25,865–25,872.
Baragiola, R.A., Atteberry, C.L., Bahr, D.A., Peters, M., 1999. J. Geophys. Res. E 104, 14,183–14,187.
Baragiola, R.A., Atteberry, C.L., Dukes, C.A., Famá, M., Teolis, B.D., 2002. Nucl. Instrum. Methods Phys. Res. B 193, 720–726.
Baragiola, R.A., Vidal, R., Shi, M., Svendsen, W., Schou, J., Bahr, D., 2003. Nucl. Instrum. Methods Phys. Res., in press.
Baratta, G.A., Leto, G., Spinella, F., Strazzulla, G., Foti, G., 1991. Astron. Astrophys. 252, 421–424.
Baratta, G.A., Castorina, A.C., Leto, G., Palumbo, M.E., Spinella, F., Strazzulla, G., 1994. Planet. Space Sci. 42, 759–766.
Bar-Nun, A., Owen, T., 1998. In: Schmitt, B., De Bergh, C., Festou, M. (Eds.), Solar System Ices. Kluwer, Dordrecht, pp. 353–366.
Bar-Nun, A., Herman, G., Laufer, D., Rappaport, M.L., 1985a. Icarus 63, 317–332.
Bar-Nun, A., Herman, G., Rappaport, M.L., Mekler, Yu., 1985b. Surf. Sci. 150, 143–156.
Bertie, J.E., Labbe, H.J., Whalley, E., 1969. J. Phys. Chem. 50, 4501–4520.
Brown, D.E., George, S.M., Huang, C., Wong, E.K.L., Rider, K., Smith, R.S., Kay, B., 1996. J. Phys. Chem. 100, 4988–4995.
Brown, W.L., Lanzerotti, L.J., Poate, J.M., Augustyniak, W.M., 1978. Phys. Rev. Lett. 40, 1027–1030.
Buch, V., 1992. J. Chem. Phys. 96, 3814–3823.
Carlson, R.W., Anderson, M.S., Johnson, R.E., Smythe, W.D., Hendrix, A.R., Barth, C.A., Soderblom, L.A., Hansen, G.B., McCord, T.B., Dalton, J.B., Clark, R.N., Shirley, J.H., Ocampo, A.C., Matson, D.L., 1999. Science 283, 2062–2064.
Devlin, J.P., 1990. Int. Rev. Phys. Chem. 9, 29–65.
Dohnálek, Z., Ciolli, R.L., Kimmel, G.A., Stevenson, K.P., Smith, R.S., Kay, B.D., 2000. J. Chem. Phys. 110, 5489–5492.
Dowell, L.G., Rinfret, A.P. 1960. Nature 158, 1144–1148.
Drobyshev, A.S., 1996. Low Temp. Phys. 22, 123–128.
Drobyshev, A.S., Garipoglyi, D.N., 1996. Low Temp. Phys. 22, 812–816.
Drobyshev, A.S., Atapina, N.V., Garipogly, D.N., Maksimov, S.L., Samyshkin, E.A., 1993. Low Temp. Phys. 19, 404–406.
Dubochet, J., Lepault, J., 1984. J. Phys. (Paris) 45, C7–85–C7-94.
Eldrup, M., Vehanen, A., Schulz, P.J., Lynn, K.G., 1985. Phys. Rev. B 32, 7048–7064.
Essmann, U., Geiger, A., 1995. J. Chem. Phys. 103, 4678–4692.
Fisher, M., Devlin, J.P., 1995. J. Phys. Chem. 99, 11,584–11,590.
Gerakines, P.A., Schutte, W.A., Ehrenfreund, P., 1996. Astron. Astrophys. 312, 289–305.
Giering, T., Haarer, D., 1996. J. Lumin. 66& 67, 299–304.
Givan, A., Loewenschuss, A., Nielsen, C.J., 1997. J. Phys. Chem. B 101, 8696–8706.
Grundy, W.M., Buie, M.W., Stansberry, J.A., Spencer, J.R., Schmitt, B., 1999. Icarus 142, 536–549.
Hagen, W., Tielens, A.G.G.M., Greenberg, 1981. Chem. Phys. 56, 367–379.
Hagen, W., Tielens, A.G.G.M., Greenberg, J.M., 1983. Astron. Astrophys. (Suppl. 51), 389–416.
Hallbrucker, A., Mayer, E., Johari, G.P., 1989. J. Phys. Chem. 93, 4986–4990.
Handa, Y.P., Mishima, O., Whalley, E., 1986. J. Chem. Phys. 84, 2766–2770.
Hapke, B., 1983. Theory of Reflectance and Emittance Spectroscopy. Cambridge University Press, Cambridge.
Heide, H.G., 1982. Ultramicroscopy 7, 299–300.
Heide, H.G., 1984. Ultramicroscopy 14, 271–278.
Heide, H.G., Zeitler, Z., 1985. Ultramicroscopy 16, 151–160.
Hessinger, J., White Jr., B.E., Pohl, R.O., 1996. Planet. Space Sci. 44, 937–944.
Horimoto, N., Kato, H.S., Kawai, M., 2002. J. Chem. Phys. 116, 4375–4378.
Hudgins, D.M., Sandford, S.A., Allamandola, L.J, Tielens, A.G.G.M., 1993. Astrophys. J. (Suppl. 86), 713–870.
Hudson, R.L., Moore, M.H., 1992. J. Phys. Chem. 96, 6500–6504.
Hudson, R.L., Moore, M.H., 1995. Radiat. Phys. Chem. 45, 779–789.
Jenniskens, P., Blake, D.F., 1994. Science 265, 753–756.

Jenniskens, P., Blake, D.F., 1996. Astrophys. J. 473, 1104–1113.
Jenniskens, P., D.F., Wilson, M.A., Pohorille, A., 1995. Astrophys. J. 455, 389–401.
Jenniskens, P., Barnhak, S.F., Blake, D.F., McCoustra, M.R.S., 1997. J. Chem. Phys. 107, 1232–1241.
Johari, G.P., Hallbrucker, A., Mayer, E., 1987. Nature 330, 552–553.
Johari, G.P., Hallbrucker, A., Mayer, E., 1991. J. Chem. Phys. 95, 2955–2964.
Johnson, R.E., 1998. In: Schmitt, B., De Bergh, C., Festou, M. (Eds.), Solar System Ices. Kluwer, Dordrecht, pp. 303.
Johnson, R.E., Jesser, W.A., 1997. Astrophys. J. 480, L79–L82.
Johnson, R.E., Quickenden, T.I., 1997. J. Geophys. Res. 102, 10,985–10,996.
Kimmel, G.A., Orlando, T.M., Vesina, C., Sanche, L. 1994. J. Chem. Phys. 101, 3282–3286.
Kimmel, G.A., Dohnálek, Z., Stevenson, K.P., Smith, R.S., Kay, B.D., 2001. J. Chem. Phys. 114, 5295–5303.
Kohl, I., Mayer, E., Hallbrucker, A., 2000. Phys. Chem. Chem. Phys. 2, 1579–1586.
Kouchi, A., 1987. Nature 330, 550–552.
Kouchi, A., Kuroda, T., 1990. Nature 344, 134–135.
Kouchi, A., Greeenberg, J.M., Yamamoto, T., Mukai, T., 1992. Astrophys. J. 388, L73–L76.
Langel, W., Fleger, H.W., Knözinger, E., 1994. Ber. Bunsenges. Phys. Chem. 98, 81–91.
La Spisa, S., Waldheim, M., Lintemoot, J., Thomas, T., Naff, J., Robinson, M., 2001. J. Geophys. Res. 106, 33,351–33,361.
Laufer, D., Kochavi, E., Bar-Nun, A., 1987. Phys. Rev. B 36, 9219–9227.
Léger, A., Gauthier, S., Défourneau, D., Rouan, D., 1983. Astron. Astrophys. 117, 164–169.
Leto, G., Baratta, G.A., 2003. Astron. Astrophys. 397, 7–13.
Leto, G., Palumbo, M.E., Strazzulla, G., 1996. Nucl. Instrum. Methods B 116, 49–52.
Mayer, E., Pletzer, R., 1986. Nature 319, 298–301.
Mishima, O., Calvert, L.D., Whalley, E., 1984. Nature 310, 393–394.
Mitlin, S., Leung, K.T., 2002. J. Phys. Chem. 106, 6234–6247.
Moore, M.H., Hudson, R.L., 1992. Astrophys. J. 401, 353–360.
Moore, M.H., Hudson, R.L., 1993. Astron. Astrophys. Suppl. Ser. 103, 45–56.
Moore, M.H., Hudson, R.L., 2000. Icarus 145, 282–288.
Moore, M.H., Ferrante, R.F., Hudson, R.L., Nuth, J.A., Donn, B., 1994. Astrophys. J. 428, L81–L84.
Moore, M.H., Hudson, R.L., Gerakines, P.A., 2001. Spectrochim. Acta A57, 843–858.
Olander, D., Rice, S.A., 1972. Proc. Natl. Acad. Sci. USA 69, 98–100.
Plonka, A., Szajdzinska-Pietek, W., Bednarek, J., Hallbrucker, A., Mayer, E., 2000. Phys. Chem. Chem. Phys. 2, 1587–1593.
Pugh, D., 2002. M.Sc. Thesis, University of Virginia.
Rowland, B., Fisher, M., Devlin, J.P., 1991. J. Chem. Phys. 95, 1378–1384.
Rowntree, P., Parenteau, L., Sanche, L., 1991. J. Chem. Phys. 94, 8570–8576.
Sack, N.J., Baragiola, R.A., 1993. Phys. Rev. B 48, 9973–9978.
Sack, N.J., Boring, J.W., Johnson, R.E., Baragiola, R.A., Shi, M., 1991. J. Geophys. Res. 96, 17,535–17,539.
Sceats, M.G., Rice, S.A., 1982. In: Franks, F. (Ed.), Water, a Comprehensive Treatise, Vol. 7. Plenum, New York (Chapter 2).
Schmitt, B., Ocampo, J., Klinger, J., 1987. J. Phys. (Paris) 48, C1, 519–525.
Schmitt, B., Espinasse, S., Grim, R.J.A., Greenberg, J.M., Klinger, J., 1989. ESA SP-302, 65–69.
Schmitt, B., De Bergh, C., Festou, M. (Eds.), 1998a. Solar System Ices. Kluwer, Dordrecht.
Schmitt, B., Quirico, E., Trotta, F., Grundy, W.M., 1998b. In: Schmitt, B., De Bergh, C., Festou, M. (Eds.), Solar System Ices. Kluwer, Dordrecht, pp. 199–240.
Schriver-Mazzuoli, L., Schriver, A., Hallou, A., 2000. J. Mol. Struct. 554, 289–300.
Shi, M., Baragiola, R.A., Grosjean, D.E., Johnson, R.E., Jurac, S., Schou, J., 1995. J. Geophys. Res. 100, 26,387–26,395.
Sieger, M.T., Simpson, W.C., Orlando, T.M., 1998. Nature 394, 554–556.
Smith, R.G., Robinson, G., Hyland, A.R., Carpenter, G.I., 1994. Mon. Not. R. Astron. Soc. 271, 481–489.
Smith, R.S., Huang, C., Wong, E.K.L., Kay, B.D., 1996. Surf. Sci. 367, L13–L18.
Spencer, J.R., Calvin, W.M., Person, M.J., 1995. J. Geophys. Res. 100, 19,049–19,056.
Stevenson, K.P., Kimmel, G.A., Dohnálek, Z., Smith, R.S., Kay, B.D., 1999. Science 283, 1505–1507.
Strazzulla, G., Torrisi, L., Foti, G., 1988. Europhys. Lett. 7, 431–434.
Trakhtenberg, S., Naaman, R., Cohen, S.R., Benjamin, I., 1997. J. Phys. Chem. B 101, 5172–5176.
Tsekouras, A.A., Iedema, M.J., Cowin, J.P., 1998. Phys. Rev. Lett. 80, 5798–5801.
Tulk, C.A., Benmore, C.J., Urquidi, J., Klug, D.D., Neuefeind, J., Tomberli, B., Egelstaff, P.A., 2002. Science 297, 1320–1323.
Verbiscer, A., Helfenstein, P., 1998. In: Schmitt, B., De Bergh, C., Festou, M. (Eds.), Solar System Ices. Kluwer, Dordrecht, pp. 157–197.
Vichnevetski, E., Bass, A.D., Sanche, L., 2000. J. Chem. Phys. 113, 3874–3881.
Vidal, R.A., Bahr, D., Baragiola, R.A., Peters, M., 1997. Science 276, 1839–1842.
Wagner, A.J., Vecitis, C., Fairbrother, D.H., 2002. J. Phys. Chem. B 106, 4432–4440.
Westley, M.S., Baragiola, R.A., Johnson, R.E., Baratta, G.A., 1995a. Nature 373, 405–407.
Westley, M.S., Baragiola, R.A., Johnson, R.E., Baratta, G.A., 1995b. Planet. Space Sci. 43, 1311–1315.
Westley, M.S., Baratta, G.A., Baragiola, R.A., 1998. J. Chem. Phys. 108, 3321–3326.
White, B.E., Hessinger, J., Pohl, R.O., 1998. J. Low Temp. Phys. 111, 233–246.
Wojcik, M.J., Buch, V., Devlin, J.P., 1993. J. Chem. Phys. 99, 2332–2344.
Wood, B.E., Roux, J.A., 1982. J. Opt. Soc. Am. 72, 720–728.
Zhdanov, V.P., Norton, P.R., 2000. Surf. Sci. 449, L228–L234.